NIH Public Access
Author Manuscript
Neuron. Author manuscript; available in PMC 2012 June 9.

Published in final edited form as:
Neuron. 2011 June 9; 70(5): 939–950. doi:10.1016/j.neuron.2011.04.020.

Lhx6 and *Lhx8* Coordinately Induce Neuronal Expression of *Shh* that Controls the Generation of Interneuron Progenitors

Pierre Flandin[1], **Yangu Zhao**[2], **Daniel Vogt**[1], **Juhee Jeong**[1], **Jason Long**[1,3], **Gregory Potter**[1], **Heiner Westphal**[2], and **John L.R. Rubenstein**[1,*]

[1]Department of Psychiatry and the Nina Ireland Laboratory of Developmental Neurobiology, University of California, San Francisco, San Francisco, CA 94158-2324, USA

[2]Laboratory of Mammalian Genes and Development, Program in Genomics of Differentiation, Eunice Kennedy Shriver National Institute of Child Health and Human Development, Bethesda, MD 20892, USA

SUMMARY

Lhx6 and *Lhx8* transcription factor coexpression in early-born MGE neurons is required to induce neuronal *Shh* expression. We provide evidence that these transcription factors regulate expression of a *Shh* enhancer in MGE neurons. *Lhx6* and *Lhx8* are also required to prevent *Nkx2-1* expression in a subset of pallial interneurons. *Shh* function in early-born MGE neurons was determined by genetically eliminating *Shh* expression in the MGE mantle zone (MZ). This mutant had reduced SHH signaling in the overlying progenitor zone, which led to reduced *Lhx6*, *Lhx8*, and *Nkx2-1* expression in the rostrodorsal MGE and a preferential reduction of late-born somatostatin$^+$ and parvalbumin$^+$ cortical interneurons. Thus, *Lhx6* and *Lhx8* regulate MGE development through autonomous and nonautonomous mechanisms, the latter by promoting *Shh* expression in MGE neurons, which in turn feeds forward to promote the developmental program of the rostrodorsal MGE.

INTRODUCTION

The medial ganglionic eminence (MGE) is a progenitor domain within the embryonic basal ganglia that generates projection neurons, such as those in the globus pallidus (GP) and interneurons of the striatum and pallium (Marín and Rubenstein, 2001; Wonders and Anderson, 2006; Batista-Brito and Fishell, 2009). Induction and early patterning of the MGE depends on the NKX2-1 and SIX3 homeodomain proteins (Sussel et al., 1999; Geng et al., 2008; Flandin et al., 2010) which lie upstream of a cascade of other transcription factors (including LHX6, LHX8, and SOX6) and secreted proteins (e.g., SHH) that promote cell type specification and differentiation (Sussel et al., 1999; Xu et al., 2005; Gulacsi and Anderson, 2006; Azim et al., 2009; Batista-Brito et al., 2009; Flandin et al., 2010; Xu et al., 2010).

The Lhx6 and Lhx8 LIM-homeodomain transcription factors have very similar expression patterns from the earliest stages of MGE development (Lavdas et al., 1999; Sussel et al., 1999; Marín et al., 2000; Flames et al., 2007; García-López et al., 2008; Fragkouli et al., 2009; herein). At early developmental stages (E10.5–E11.5), *Lhx6* null mutant mice have

*Correspondence: john.rubenstein@ucsf.edu.
[3]Present Address: Genentech, South San Francisco, CA 94080, USA

SUPPLEMENTAL INFORMATION Supplemental Information includes six figures, three tables, and Supplemental Experimental Procedures and can be found with this article online at doi:10.1016/j.neuron.2011.04.020.

NIH-PA Author Manuscript
NIH-PA Author Manuscript
NIH-PA Author Manuscript

NIH-PA Author Manuscript

NIH-PA Author Manuscript

NIH-PA Author Manuscript

reduced numbers of pallial interneurons and very few that express somatostatin or parvalbumin (Alifragis et al., 2004; Liodis et al., 2007; Zhao et al., 2008). *Lhx6* also promotes the rate of tangential migration of interneurons (Alifragis et al., 2004; Liodis et al., 2007; Zhao et al., 2008). In the *Lhx6* mutant, MGE-derived inter-neurons, detected by virtue of placental alkaline phosphatase (PLAP) expressed from the *Lhx6* locus, have abnormal intracortical laminar position and reduced expression of receptors (Cxcr4, Cxcr7, and *ErbB4*) and transcription factors (*Arx*, *Cux2*, and *Mafb*) implicated in interneuron migration and positioning (Zhao et al., 2008). *Lhx6* mutant also have reductions in subsets of striatal GABAergic interneurons (parvalbumin$^+$ and neuropeptide Y$^+$), whereas their globus pallidus appeared normal (Zhao et al., 2008).

Lhx8 null mutant have a more restricted phenotype, which is largely associated with reduced numbers of Islet1$^+$ cholinergic neurons, particularly in the striatum (Zhao et al., 2003; Mori et al., 2004; Fragkouli et al., 2005; Fragkouli et al., 2009). In the absence of *Lhx8*, progenitors of striatal cholinergic interneurons switch fate into striatal GABAergic interneurons (Fragkouli et al., 2009).

Because the *Lhx6* and *Lhx8* have very similar expression patterns and encode highly homologous proteins, it is likely that they have redundant functions. Here, we explore this by analyzing the phenotype of *Lhx6*/*Lhx8* double mutant and demonstrate that these two genes coregulate development of pallial interneurons and subpallial projections neurons (globus pallidus and septal). Importantly, *Lhx6* and *Lhx8* control MGE development through both cell-autonomous and non-cell-autonomous mechanisms. The double mutant, but not the single mutants, lacks *Shh* expression in early-born neurons of the MGE. We provide evidence that LHX6 and LHX8 directly regulate expression of a *Shh* enhancer in MGE neurons.

Next, we determined the function of *Shh* in early-born neurons of the MGE by generating a conditional mutant that deletes *Shh* in the MGE mantle zone (MZ). Surprisingly, this mutant had reduced SHH signaling in the overlying progenitor zone, which led to reduced *Lhx6*, *Lhx8* and *Nkx2-1* expression in the rostrodorsal MGE and its derivatives, including parts of the bed nucleus stria terminals, septal complex, and subsets of pallial interneurons. The reduction in somatostatin$^+$ and parvalbumin$^+$ cortical interneurons appeared to be equally sensitive to this loss of Shh. Thus, *Lhx6* and *Lhx8* regulate MGE development through autonomous and nonautonomous mechanisms; the latter by promoting *Shh* expression in MGE neurons, which in turn feeds forward to promote the developmental program of the rostrodorsal MGE.

RESULTS

Lhx6 and *Lhx8* Double Mutant (*Lhx6*$^{PLAP/PLAP}$;*Lhx8*$^{-/-}$) Had Interneuron, Globus Pallidus, Septal, Diagonal Band, and Bed Nucleus Stria Terminalis Defects

Lhx6 and *Lhx8* are coexpressed in >90% cells in the SVZ of the MGE at E11.5 (data not shown). To uncover their combined function, we studied the phenotype of *Lhx6* and *Lhx8* double null mutants (*Lhx6*$^{PLAP/PLAP}$;*Lhx8*$^{-/-}$) at E11.5, E14.5, and E18.5. We included data on the *Lhx6*$^{PLAP/PLAP}$, *Lhx8*$^{-/-}$, and compound heterozygote mutants in supplemental figures (see Figures S1, S2, and S3 available online).

We begin our analyses by following *Lhx6*-expressing cells labeled by expression of the PLAP reporter gene that was inserted into the *Lhx6* locus (Choi et al., 2005). At E11.5, PLAP staining showed that tangential interneuron migration into the LGE was reduced in the *Lhx6*$^{PLAP/PLAP}$;*Lhx8*$^{-/-}$ mutant (Figures 1A–1C′), while it was preserved in the single mutants (Figure S1; Zhao et al., 2008).

NIH-PA Author Manuscript

NIH-PA Author Manuscript

NIH-PA Author Manuscript

At E14.5, the double mutant continued to exhibit a severe reduction in $PLAP^+$ cells migrating to the neocortical marginal zone and cortical plate, although they did have migration into the neocortical SVZ (Figures 3A, 3A′, and S2). They also had reduced $PLAP^+$ cells in the paleocortex (Figures 2A–2C′). Migration into the striatum was reduced. PLAP staining in the region of the globus pallidus was abnormal; rather than a well-defined pallidal nucleus, the $PLAP^+$ cells/processes were arranged in clusters/strands. There was a loss of $PLAP^+$ cells in the septum, diagonal band, anterior extension of the bed nucleus of stria terminalis (medial division; STMA) and the region of the core of the nucleus accumbens (AcbC) (data not shown). Finally, the anterior commissure failed to cross the midline (not shown).

At E18.5, the severe deficit in $Lhx6^{PLAP/PLAP}$;$Lhx8^{-/-}$ cortical interneurons persisted in the hippocampus, neocortex, and paleocortex, although some $PLAP^+$ cells remained in the cortical SVZ (Figures 3D, 3D′, and S3). A large ectopic cluster of $PLAP^+$ cells was present in the region of the dorsal MGE progenitor zone (Figures 3F, 3F′, and S3). Globus pallidus size and the expression of PLAP in the medial septum and diagonal band were greatly reduced (Figure S3). To elucidate the mechanisms underlying the defects in the migration of Lhx6-$PLAP^+$ cells, we used in situ RNA hybridization to study expression of genes that are either known to regulate MGE development or are markers of these cells.

Lhx6$^{PLAP/PLAP}$;*Lhx8*$^{-/-}$ Mutant Failed to Express *Shh* in Early-Born MGE Neurons

As early as ~24 hr after the onset of *Lhx6* and *Lhx8* expression there were profound changes in molecular properties of the E11.5 MGE in $Lhx6^{PLAP/PLAP}$;$Lhx8^{-/-}$ mutant; these were more severe than in the single mutants (Zhao et al., 2008, and data not shown). The most salient feature was the loss of *Shh* expression in the MGE mantle zone (arrows, Figures 1E and 1E′); its VZ expression was preserved (arrowheads, Figures 1E and 1E′). There was an ~50% reduction in *Ptc1* and *Nkx6-2* expression in the MGE VZ, particularly in dorsal regions (arrows, Figures 1H and 1H′ and Figures 1L and 1L′; Table S1); *Ptc1* and *Nkx6-2* expression are positively regulated in the MGE by SHH signaling (Xu et al., 2005, 2010). In addition, there was a strong reduction of *Nkx2-1* expression in the dorsal-most MGE (arrows, Figures 1N and 1N′). Expression of other major regulators (*Dlx2* and *Nkx2-1*), or markers (*Inhibin beta* [*activin beta A*], *Er81*, *Islet1*, and *Zic1*) of MGE development were not greatly altered at E11.5 (Figure S1), although there was reduced *Er81* expression in the MZ (Figure S1).

Thus, SHH produced by postmitotic MGE neurons may promote *Ptc1*, *Nkx6-2*, and *Nkx2-1* expression in the overlying ventricular zone. Later in the paper, we demonstrate the function of Shh that is expressed in these MGE neurons.

Lhx6&8 Promoted *Lmo3* and *Nkx2-1* Expression in MGE Progenitors and Development of the Globus Pallidus at E14.5 and E18.5

At E14.5 *Nkx2-1* expression in the VZ of the double mutant persisted in most regions of the basal ganglia, except in the rostral MGE and septum (arrows, Figures 2D and 2D′). This region also showed reduced *Gli1* and *Nkx6-2* expression (arrows, Figures 2G and 2G′, and not shown). The double mutant also had reduced SVZ expression of *Lmo3* and *Nkx2-1* (arrows, Figures 2D and 2D′ and Figures 2L and 2K′), which was not noted in the single mutants (Figure S2; Zhao et al., 2008). There was not a general defect of the MGE SVZ, as expression of *Arx*, *Dlx1*, *Gad1*, *Lhx6* (PLAP), and SOX6 were preserved (arrows, Figures 2B and 2B′, 2N and 2N′, and S2); persistence of *Lhx6* (PLAP) and SOX6 expression showed that the SVZ maintained aspects of its MGE fate. *Arx* expression may be increased in the SVZ of the MGE of the $Lhx8^{-/-}$ mutant (Figure S1).

NIH-PA Author Manuscript

NIH-PA Author Manuscript

NIH-PA Author Manuscript

MZ defects were prominent in the double mutant, particularly with the loss of a well-defined globus pallidus. While *Zic1* and *Er81* continued to be expressed in a loosely organized globus pallidus, other markers did not coalesce into a globus pallidus (*Arx*, *Dlx1*, *Lmo3*, *Nkx2-1*, and SOX6) (Figures 2F and 2F′, 2L, and 2L′, 2O and 2O′, and S2). Similar globus pallidus defects were seen at E18.5 (Figures 3F, 3F′, and S3). The phenotype was much more severe than in either single or compound heterozygote mutant, except for Npas1 expression, which appeared similar to the $Lhx6^{PLAP/PLAP}$ mutant.

At E18.5 the progenitor zone of the rostrodorsal MGE and the adjacent part of the septum exhibited reduced expression of *Nkx2-1* and PLAP in the $Lhx6^{PLAP/PLAP}$;$Lhx8^{-/-}$ mutant (Figure S3). Presumptive derivatives of this region (medial septum and diagonal band) showed reduced numbers of cells expressing *Nkx2-1*, PLAP, and SOX6 (Figure S3). In addition, the bed nucleus stria terminalis had reduced expression of Calbindin in both the $Lhx6^{PLAP/PLAP}$ and $Lhx6^{PLAP/PLAP}$;$Lhx8^{-/-}$, whereas *Dlx1* and *Gad1* expression were maintained (Figure S3 and not shown).

Striatal and Cortical Interneuron Defects in $Lhx6^{PLAP/PLAP}$;$Lhx8^{-/-}$ Mutant

Interneurons tangentially migrating to, and into, the cortex were reduced in the $Lhx6^{PLAP/PLAP}$;$Lhx8^{-/-}$ mutant at E14.5 and E18.5 (Figures 3, S2, and S3). At E14.5, the double mutant striatum had reduced numbers of Som^+, $SOX6^+$, and $Zic1^+$ interneurons (Figures 2 and S2). At E18.5, the $Lhx6^{PLAP/PLAP}$;$Lhx8^{-/-}$ mutant striatum had an ~50% reduction of $NKX2\text{-}1^+$, som^+, and $SOX6^+$ cells, an ~95% reduction of Npy^+ cells and no reduction in $Npas1^+$ cells, when compared with double heterozygote controls (Figure S3; Table S2). The pallium (endopiriform nucleus, claustrum, piriform pallial amygdala, cortex, neocortex, and hippocampus) had reduced numbers of interneurons expressing *Arx*, Calbindin, *Gad1* (*Gad67*), *Npas1*, PLAP (*Lhx6*), *Som*, and SOX6, compared with double heterozygote controls (Figures 2, 3, S2, and S3; not shown). However, PLAP was the only marker that was clearly more reduced in the $Lhx6^{PLAP/PLAP}$;$Lhx8^{-/-}$ mutant compared to the $Lhx6^{PLAP/PLAP}$ mutant (Figures S2 and S3; Table S2).

Defects in migration may have contributed to the reduced numbers of striatal and pallidal interneurons. There were increased numbers of scattered subpallial $Nkx2\text{-}1^+$, Som^+, and $SOX6^+$ cells, particularly in caudal regions of the basal ganglia (arrowheads, Figures 2F and 2F′, 2O and 2O′, S2, and S3). Furthermore, many $PLAP^+$ cells failed to migrate from the MGE; these formed a large collection of cells in the SVZ of the dorsal MGE (ectopia [E]; Figures 3F and 2F′). The cells in the ectopia expressed *Dlx1 and Gad1* and did not express *Nkx2-1*, Calbindin, and SOX6, suggesting that they had properties of the LGE/dCGE rather than the MGE (Figure S3). The $Lhx6^{PLAP/PLAP}$;$Lhx8^{-/-}$ MGE ectopia was much more prominent than in $Lhx6^{PLAP/PLAP}$ mutant (Zhao et al., 2008). Like the $Lhx6^{PLAP/PLAP}$ mutant, the double mutant continued to have tangentially migrating interneurons expressing *Arx*, *Dlx1*, and *Gad1* (Figures S2 and S3) presumably originating from the LGE/dCGE.

Normally, *Nkx2-1* expression is maintained only in interneurons migrating to the striatum and projection neurons of the basal telencephalon and septum (Marín et al., 2000; Marín and Rubenstein, 2001; Nóbrega-Pereira et al., 2008). However, at E14.5 there were ectopic $Nkx2\text{-}1^+$ cells in the caudal regions of the external capsule (arrow) and ventrolateral cortex in the $Lhx6^{PLAP/PLAP}$ and $Lhx6^{PLAP/PLAP}$;$Lhx8^{-/-}$ mutant and increased numbers in the striatum (arrowhead, Figures 3C, 3C′, and S2). By E18.5 there were ectopic $NKX2\text{-}1^+$ cells in the cortical SVZ and the hippocampus of the $Lhx6^{PLAP/PLAP}$, $Lhx6^{PLAP/PLAP}$;$Lhx8^{+/-}$, and $Lhx6^{PLAP/PLAP}$;$Lhx8^{-/-}$ mutant (Figures 3G, 3G′, and S3). They were most prevalent in the $Lhx6^{PLAP/PLAP}$;$Lhx8^{+/-}$ mutant, which also had increased numbers of $NKX2\text{-}1^+$ cells in the SVZ of the LGE (data not shown), suggesting that these cells were in transit along their migration from the MGE to the cortex. Thus, *Lhx6* and *Lhx8* are required to prevent

NIH-PA Author Manuscript

NIH-PA Author Manuscript

NIH-PA Author Manuscript

NKX2-1 expression in pallial interneurons. The ectopic NKX2-1^{+} cells accumulated in stratum radiatum of the hippocampus; this region also accumulated cells expressing *Lhx6*-PLAP, Calbindin, *Dlx1*, *Gad1*, and *Npas1*, but did not express SOX6 (Figures 3G, 3G′, and S3). Because the mutants die at P0, we have not identified their identity at maturity.

Deletion of Shh Expression from MGE Mantle Zone Neurons (*Dlx1/2-cre;Shh$^{F/-}$*) Reduced Shh Signaling in MGE Progenitors The phenotype of the

The phenotype of the *Lhx6$^{PLAP/PLAP}$;Lhx8$^{-/-}$* mutant is probably the combination of cell autonomous defects in cells lacking these transcription factors and cell nonautonomous effects due to the loss of *Shh* expression in the MZ of the MGE (Figure 1). While the effect of removing *Shh* expression from the VZ of the MGE/POA has been established to alter properties of MGE progenitors (Gulacsi and Anderson, 2006; Xu et al., 2005, 2010), the function of *Shh* in postmitotic neurons of the MGE is unknown.

Shh is transiently expressed in most MGE neurons from ~E10–E12 (Figures 1A–1C; Sussel et al., 1999; Flandin et al., 2010). To determine its function in these cells we induced a deletion of *Shh* exon 2 using a floxed *Shh* allele (Dassule et al., 2000; Lewis et al., 2004) and *Dlx I12b-Cre*. The *Dlx I12b-cre* allele is expressed in SVZ and MZ, but not the VZ, of the basal ganglia, beginning around E10.5 (Potter et al., 2009). We refer to this mutant as *Dlx1/2-cre;Shh$^{F/-}$*. The *Dlx1/2-cre;Shh$^{F/-}$* mutant lacked expression of *Shh* exon 2 RNA and SHH protein (in the MGE MZ [arrows, Figures 4B, 4B′, 4C, and 4C′], but not in the VZ [arrowheads, Figures 4B, 4B′, 4C, and 4C′, and not shown]). On the other hand, *Shh* transcripts continued to be expressed in the *Dlx1/2-cre;Shh$^{F/-}$* MGE MZ (Figures 4D−4F′), showing that *Shh* expression in these cells does not require continued production of Shh protein, and that this cell type was present.

At E11.5, the *Dlx1/2-cre;Shh$^{F/-}$* exhibited reduced MGE SHH signaling based on ~2-fold decreased *Gli1*, *Ptc1*, and *Nkx6-2* expression in the VZ and SVZ of the overlying MGE MZ compared to control brains (*Cre^{-};Shh$^{F/-}$ or Cre^{-};Shh$^{F/+}$*) (Figures 4 and S4; Table S1), thus showing that *Shh* expression in postmitotic neurons regulates properties of MGE progenitor cells. These effects were prominent in the dorsal MGE, where *Gli1* and *Nkx6-2* expression were strongly reduced (arrows, Figures 4K, 4J′, 4N, and 4M′). *Ptc1*, *Gli1*, and *Nkx6-2* expression in the ventral-most MGE and preoptic area appeared normal, presumably because *Shh* expression in the VZ was not affected. Surprisingly, NKX2-1 expression was largely unchanged, except for the loss of expression in the VZ of the dorsal-most MGE (arrows, Figures 4Q and 4Q′). Furthermore, the mutant's MGE did not show an obvious morphological change.

The *Dlx1/2-cre;Shh$^{F/-}$* Mutant Had Abnormal Progenitor Specification and Differentiation in the Rostrodorsal MGE

The *Dlx1/2-cre;Shh$^{F/-}$* mutation preferentially altered differentiation in the rostrodorsal MGE at E14.0 (Figure 5). *Ptc1* expression in the VZ of this region was greatly reduced, whereas its expression in the preoptic area remained strong (Figure S5). Likewise, expression of *Gli1*, *Lhx6*, *Lhx8*, *Nkx2-1*, and *Nkx6-2* in the VZ, SVZ, and MZ were selectively reduced in the rostrodorsal MGE (arrows, Figures 5 and S5). Consistent with this, properties of the mutant's globus pallidus appeared unchanged (*Er81*, *Lhx6*, *Lhx8*, *Nkx2-1*, and *Zic1*; Figure S5), as the globus pallidus is largely derived from the ventral MGE and dorsal preoptic area (Flandin et al., 2010; Nóbrega-Pereira et al., 2010).

The rostrodorsal MGE of the *Dlx1/2-cre;Shh$^{F/-}$* mutant had strong phenotypes at E18.5 (Figures 6 and S6). This area includes the region of the anterior extension of the bed nucleus of stria terminalis (medial division; STMA) and the core of the nucleus accumbens (AcbC).

NIH-PA Author Manuscript

NIH-PA Author Manuscript

NIH-PA Author Manuscript

These regions lacked detectable expression of *Lhx6*, *Lhx8*, and *Nkx2-1* in the progenitor zone and showed reduced expression in the mantle zone (arrows, Figure 6); *Lhx6* expression in tangentially migrating cells coursing through the LGE SVZ was also reduced (arrowheads, Figures 6C and 6C′). On the other hand, expression of *Islet1* in the AcbC appeared normal (Figure S6). Striatal expression of *Islet1* adjacent to the LGE progenitor domain appeared reduced.

Septal and diagonal band neurons of the *Dlx1/2-cre;Shh*$^{F/-}$ mutant had molecular defects (Figures 6 and S6). The lateral septum showed reduced *Nkx2-1*, while expression of *Zic1* and *Islet1* appeared normal. The diagonal band complex (VDB/HBD) had reduced expression of *Nkx2-1*, *Lhx6*, and *Lhx8*. On the other hand, the medial septum showed normal expression of *Lhx6* and *Lhx8*. Also, pallidal regions were not affected in the *Dlx1/2-cre;Shh*$^{F/-}$ mutant, as expression of *Lhx6*, *Lhx8*, and *Zic1* appeared normal in the ventral pallidum and substantia inmoninata, and *Lhx6*, *Lhx8*, *Lmo3*, *Nkx2-1*, *Npas1*, SOX6, and *Zic1* appeared normal in the globus pallidus (Figures 6 and S6). Finally, the anterior commissure appeared normal (Figure 6).

The MGE of *Dlx1/2-cre;Shh*$^{F/-}$ mutant had increased apoptosis and possibly a reduction in proliferation. We found no clear proliferation defect at E11.5, E14.0, and E15.5, as judged by the number of PH3^{+} mitotic nuclei (Figures S4 and S5 and data not shown), consistent with *Shh*;*Nestin-Cre* conditional mutant (Xu et al., 2005). On the other hand, by E18.5, in the rostrodorsal MGE, there was a trend for a reduction in PH3^{+} cells (~50%; p = 0.07; Figure S6). In addition, was an increase in the number of apoptotic cells (activated caspase-3^{+}) in the MGE at E14.0, E15.5, and E18.5 (Figures S5 and S6 and data not shown), consistent with the *Nestin-cre* deletion of *Smoothened* (SHH signaling component) (Machold et al., 2003). Given the molecular and cellular defects in the rostrodorsal MGE and its derivatives, we investigated the effect of the *Dlx1/2-cre;Shh*$^{F/-}$ mutation on the number and nature of cortical interneurons.

Dlx1/2-cre;Shh$^{F/-}$ Mutant Had Reduced Numbers of Cortical Interneurons

At E14.0 we did not detect a reduction in the number of Calbindin^{+} and *Lhx6*$^{+}$ cells in the cortex (Figures 7A and 7A′; data not shown; Table S3). However, by E18.5, the *Dlx1/2-cre;Shh*$^{F/-}$ cortical plate had fewer interneurons expressing Calbindin (50% reduction), *Lhx6* (40% reduction), *Npas1* (20% reduction), and SOX6 (23% reduction) (Figures 7B, 7B′, and S6; data not shown; Table S3). The E18.5 striatum had roughly normal numbers of *Lhx6*$^{+}$, *Lhx8*$^{+}$, NKX2-1^{+}, and SOX6^{+} interneurons, and ~30% reduction of *Som*$^{+}$ interneurons (Figures 6 and S6; Table S3).

The *Dlx1/2-cre;Shh*$^{F/-}$ mutant survived postnatally to at least P24, although they were smaller than control littermates (heterozygote: 16.48 ± 0.34 g; mutant: 8.10 ± 1.10 g; p = 0.0019), enabling us to evaluate the number and nature of their cortical interneurons subtypes (n = 3 animals for each genotype). We counted the number of interneurons expressing the CR, NPY, PV, and SOM. Consistent with the reduction in *Lhx6* expression, we found reductions of CR^{+}, PV^{+}, and SOM^{+} cortical interneurons (Figure 7), the cell types reduced in the *Lhx6* mutant (Liodis et al., 2007; Zhao et al., 2008). The PV^{+} and SOM^{+} subtypes were similarly reduced (~40% in superficial layers and ~20% in deep layers); CR^{+} interneurons were slightly more affected (~40% in superficial layers and ~35% in deep layers; Figure 7K). Of note, we detected no difference in the number of PV^{+} interneurons in the hippocampus (data not shown).

At P24, the mutant had an ~15% reduction in the number of striatal PV^{+} interneurons; no statistically significant difference was observed in the number of striatal interneurons expressing CR, NPY, or SOM (Table S3).

NIH-PA Author Manuscript

NIH-PA Author Manuscript

NIH-PA Author Manuscript

LHX6 and LHX8 Bind to and Activate Transcription From the *Shh* MGE Enhancer

We demonstrated that the *Lhx6*$^{PLAP/PLAP}$;*Lhx8*$^{-/-}$ mutant fails to express *Shh* in early-born MGE MZ neurons (Figure 1). To investigate whether LHX6 and/or LHX8 can directly regulate *Shh* expression we utilized a 384 bp enhancer element (SBE3) from the *Shh* locus that drives expression in the MGE MZ at E10.5 (Figure 8A; Jeong et al., 2006). Using a bioinformatic approach (see Supplemental Experimental Procedures), we identified one putative LHX binding site in the SBE3 enhancer (site A; Figure 8A). Electrophoretic mobility shift assay (EMSA) showed that both LHX6 and LHX8 bind to SBE3; binding was greatly reduced when LHX site A was mutated (Figures 8B and 8C).

Next, we cloned SBE3 upstream of a minimal promoter and the mCherry coding sequence. We tested whether *Lhx6* and/or *Lhx8* promoted reporter gene expression in primary cultures from E12.5 MGE. mCherry^{+} cells were detected by immunofluorescence. *Lhx6*, *Lhx8*, and *Lhx6*&*8* increased mCherry expression roughly 3- to 4-fold ($n = 4$, $p < 0.05$; Figure 8D). On the other hand, when wild-type SBE3 was replaced with mutant SBE3 (site A), there was a ~2.5-fold reduction in activation by *Lhx6* and *Lhx6*&*8* ($p < 0.05$); there was a similar trend for *Lhx8* reduction, but it was not statistically significant ($n = 4$; Figure 8D). Therefore, these results provide evidence that *Lhx6* and *Lhx8* can activate transcription in part through the LHX-binding site A in SBE3.

DISCUSSION

Redundant Functions of *Lhx6* and *Lhx8*

Lhx6 and *Lhx8* each has prominent individual functions in regulating the development of GABAergic and cholinergic neurons generated in the MGE (Zhao et al., 2003, 2008; Mori et al., 2004; Alifragis et al., 2004; Fragkouli et al., 2005, 2009; Liodis et al., 2007). Here, by analyzing mice lacking both genes we demonstrated that *Lhx6* and *Lhx8* also have redundant functions. A key early redundant function is to promote *Shh* expression in neurons of the MGE mantle zone (Figure 1); SHH production by these cells then regulates the properties of the overlying SHH-negative MGE progenitor zone, including the expression of *Gli1*, *Nkx6-2* and *Ptc1* (Figure 8E). Later in this discussion, we will expand upon the function of *Shh* expression in the MGE neurons.

Lhx6 and *Lhx8* together regulate the molecular properties of the MGE SVZ; the double mutant showed reduced expression of the *Lmo3* and *Nkx2-1* transcription factors that was greater than in the single mutants (Figures 2 and S2). *Nkx2-1* is essential in the VZ to specify MGE identity (Sussel et al., 1999; Flandin et al., 2010; Butt et al., 2008), and in the SVZ it is required for development of striatal interneurons and the globus pallidus (Nóbrega-Pereira et al., 2008; P.F. and J.L.R.R., unpublished data).

Reduced *Nkx2-1* expression is likely to contribute to the abnormal globus pallidus of the *Lhx6*$^{PLAP/PLAP}$;*Lhx8*$^{-/-}$ mutant, that fails to coalesce into a nucleus expressing *Arx*, *Dlx1*, *Lhx6*, *Lmo3*, *Nkx2-1*, and SOX6 (Figures 2, S2, and S3). On the other hand, *Npas1* and *Zic1* expression in the region of the mutant's globus pallidus was preserved (Figures S2 and S3); *Npas1*$^{+}$ and *Zic1*$^{+}$ cells probably correspond to globus pallidus neurons generated from distinct regions that are independent of *Nkx2-1* and *Lhx6/Lhx8* function (Flandin et al., 2010; Nóbrega-Pereira et al., 2010). *Lhx6* and *Lhx8* are also required for generating other basal ganglia neurons, including cells in the septum, diagonal band and bed nucleus stria terminalis; the latter cells depend primarily on *Lhx6* (Figures 2, S2, and S3).

Lhx6 and *Lhx8* also share functions in the development of interneurons of the pallium and striatum. In the paleocortex, neocortex, and hippocampus, the double mutant had more severe defects than the single mutants, in the number of *Lhx6*-PLAP^{+} pallial interneurons

NIH-PA Author Manuscript

NIH-PA Author Manuscript

NIH-PA Author Manuscript

(from E11.5 to E18.5; Figures S2 and S3). There was almost no superficial migration in the marginal zone; they had a modest “deep” migration (Figures 3, S2, and S3). Thus, *Lhx8*, which is not expressed in tangentially migrating pallial interneurons, must contribute to their development through its expression in the SVZ of the MGE. *Lhx6*$^{PLAP/PLAP}$;*Lhx8*$^{-/-}$ mutant also had striatal interneuron defects that were more severe than the single mutants (Table S2); for instance, they lacked almost all NPY^{+} interneurons.

The reduced numbers of *Lhx6*-PLAP^{+} cortical interneurons in the double mutant may be due to a block in the migration of these cells from the MGE, as the *Lhx6*$^{PLAP/PLAP}$;*Lhx8*$^{-/-}$ mutant had a large ectopia in the SVZ of the dorsal MGE (Figures 3 and S3). The cells within the ectopia had an altered identity, as they expressed markers more consistent with those of the LGE/dCGE rather than the MGE. Like the LGE/dCGE they express *Dlx1* and *Gad1*, and failed to express Calbindin, *Nkx2-1*, and SOX6 (Figure S3 and not shown).

Previously, it was reported that *Lhx6* is required for *Sox6* expression in MGE-derived interneurons (Batista-Brito et al., 2009). However, strong SOX6 expression was present in the SVZ of the MGE (arrow, Figure 2) and in cells scattered throughout the mantle zone of the caudal basal ganglia (arrowhead, Figures 2, S2, and S3) in the *Lhx6*$^{PLAP/PLAP}$ and *Lhx6*$^{PLAP/PLAP}$;*Lhx8*$^{-/-}$ mutant. Furthermore, we found SOX6^{+} cells in the mutants' neocortex, although their numbers were reduced (Figures 3, S2, and S3; Table S2). Much of this reduction, especially in the double mutant, could be due to reduced numbers of MGE-derived interneurons, as suggested by the reduced cortical PLAP expression and the large PLAP^{+} ectopia in the MGE (Figures 3 and S3). Thus, in most MGE cells, induction of SOX6 expression does not require *Lhx6* and *Lhx8*. On the other hand, maintenance of SOX6 expression in cells fated to be pallial interneurons (including in the MGE ectopia) appears to be promoted by Lhx6 function, similar to the expression of *CXCR4*&*7Cxcr4*, *Cxcr7*, and *ErbB4* (Zhao et al., 2008). The double mutant also had scattered SOX6^{+} cells in the MZ of the basal ganglia (Figures 2 and 3); these may reflect interneurons that aberrantly migrated.

Lhx6, and more prominently in combination with *Lhx8*, is required to restrict NKX2-1^{+} cells to the subpallium. Mice lacking these transcription factors had ectopic pallial NKX2-1^{+} cells, particularly in the hippocampus and cortical SVZ. The interneurons in these regions of the mutant expressed markers of dCGE-derived interneurons (*Dlx1*, *Gad1*, *Npas1*, and not SOX6) (Figures 3 and S3). However, perhaps because of NKX2-1 expression, they had a mixed MGE/dCGE identity and thereby expressed Lhx6-PLAP and Calbindin (Figures 3 and S3). Ordinarily, NKX2-1 expression is extinguished as cortical interneurons leave the MGE (Marín et al., 2000; Nóbrega-Pereira et al., 2008); persistent NKX2-1 expression prevents interneurons from entering the cortex (Nóbrega-Pereira et al., 2008). However, in *Lhx6*$^{PLAP/PLAP}$;*Lhx8*$^{-/-}$ mutant NKX2-1 expression was not extinguished in some pallial interneurons. Thus, we propose that *Lhx6/Lhx8* function is required for NKX2-1 to prevent cells from migrating to the pallium (Figure 8E). Future studies are needed to establish the molecular mechanisms through which *Lhx6/Lhx8* regulate this process.

Shh Functions in MGE Neurons to Regulate the Identity, Survival, and Proliferation of the Overlying Progenitor Zone

Shh expression in the ventricular zone of the telencephalon is established in the preoptic area (POA) and ventral MGE through the actions of the *Nkx2-1* and *Six3* transcription factor genes (Figure 8E; Sussel et al., 1999; Geng et al., 2008). There, SHH promotes the expression of *Nkx2-1* in proliferating cells (Gulacsi and Anderson, 2006; Xu et al., 2005, 2010).

Shh is also expressed in postmitotic MGE neurons; these cells comprise a large fraction of the MZ at E11.5. At later stages, *Shh* expression in this region is more difficult to detect by

NIH-PA Author Manuscript

NIH-PA Author Manuscript

NIH-PA Author Manuscript

in situ hybridization (P.F. and J.L.R.R., unpublished data) but does continue throughout development and into adulthood in specific subpallial cell types and regions, including the diagonal band (P.F. and J.L.R.R., unpublished data; Allen Brain Atlas).

Here, we present the first evidence that *Shh* expression in the MGE MZ regulates the properties of the overlying MGE VZ. We selectively deleted the *Shh* gene in the MGE MZ using *Dlx1/2-Cre* (*Dlx1/2-cre*;$Shh^{F/-}$). This Cre allele is expressed in SVZ and MZ, but not the VZ, of the basal ganglia, beginning around E10.5 (Potter et al., 2009); thus, leaving *Shh* expression intact in the VZ. Removal from the MZ did not show a defect in SHH signaling in the ventral MGE, based on preserved expression of *Ptc1* and *Nkx2-1* (Figures 4 and S4). Rather, the *Dlx1/2-cre*;$Shh^{F/-}$ mutant showed a defect in SHH signaling in the dorsal and middle MGE, where expression of *Gli1*, *Ptc1*, and *Nkx6-2* were reduced at E11.5 and E14.0 (Figures 4 and S4; Table S1), which was very similar to the VZ defects found in the $Lhx6^{PLAP/PLAP}$;$Lhx8^{-/-}$ mutant (Figures 1 and S1). By E18.5, the progenitor zone phenotype in the *Dlx1/2-cre;*$Shh^{F/-}$ mutant appeared to be restricted to the rostrodorsal MGE.

We propose that *Lhx6/Lhx8*-dependent *Shh* expression and secretion from neurons in the MGE MZ regulates the properties of the overlying VZ. The Shh signaling may take place in the radial glial processes that interdigitate among the neurons, and/or through Shh diffusion to the VZ, where it would activate signaling in the neuroepithelial cell bodies.

The ramifications of reducing Shh signaling in the dorsal MGE (based on reduced *Gli1* and *Ptc1* expression) include greatly reduced VZ expression of *Nkx2-1* and *Nkx6-2* and SVZ expression of *Lhx6* and *Lhx8* (Figures 4, 5, 6, S4, and S5). As discussed throughout this paper, *Nkx2-1*, *Lhx6*, and *Lhx8* are required for the development of most MGE-derivatives. *Nkx6-2* function is required for generating a subset of SOM^+;CR^+ interneurons (Sousa et al., 2009), and *Gli1* (in conjunction with *Gli2*) is required in patterning the dorsal MGE and in generating cortical interneurons (Yu et al., 2009).

There is evidence that Shh dosage participates in the specification of cortical interneuron subtypes. Exposing MGE explants to 10 nM SHH altered the distribution of interneuron fates that are present after transplantation into a neonatal cortex; augmentation of Shh-signaling increased SOM^+ cells and reduced PV^+ cells (Xu et al., 2010). This result led to the proposal that high SHH signaling promotes SOM fate over PV fate. However, this idea does not readily fit with fate mapping data showing that the dorsal MGE has the propensity to generate SOM^+ neurons, whereas the ventral MGE, whose VZ has much higher Shh expression has the propensity to generate PV^+ neurons (Flames et al., 2007; Wonders et al., 2008; Flandin et al., 2010).

The previous in vivo investigations into Shh regulation of inter-neuron development focused on *Shh* expression and function in the VZ; here, we addressed whether *Shh* expression in the MZ of the MGE controls interneuron development. In *Dlx1/2-cre;*$Shh^{F/-}$ mutant, consistent with the reduction in *Lhx6* expression, we found reductions of SOM^+ and PV^+ cortical interneurons (Figure 7). However, both subtypes were similarly reduced (~40% in superficial layers and ~20% in deep layers), failing to provide evidence that *Shh* expression in the MZ differentially regulated interneuron fate. Rather, these results support a model that *Shh* expression in the MZ, promotes SHH signaling in the dorsal MGE that then produces both SOM^+ and PV^+ cortical interneurons. On the other hand, Shh expression in the VZ of the ventral MGE and POA is critical for regulating development of these more ventral regions.

Early-born SOM^+ and PV^+ cortical interneurons populate deep cortical layers; therefore, the 2-fold greater decrease of SOM^+ and PV^+ cortical interneurons in the superficial cortical

NIH-PA Author Manuscript

NIH-PA Author Manuscript

NIH-PA Author Manuscript

layers (Figure 7) provides evidence that *Shh* expression in the MGE MZ has increased importance in maintaining interneuron production and/or survival as development proceeds. While proliferation in the *Dlx1/2-cre;Shh*$^{F/-}$ mutant's rostrodorsal MGE appeared normal at E11.5 and E14.0 (Figures S4 and S5 and data not shown), by E18.5 there was a trend for a reduction in PH3^{+} cells (~50%; p = 0.07) (Figure S6). Furthermore, while the number cortical interneurons in the mutant appeared normal at E14.0, by E18.5, there was a clear reduction in MGE-derived interneuron numbers (Figures 7A, 7A′, 7B, 7B′, and S6; Table S3). Increased apoptosis in the mutant's MGE may have also contributed to the reduction in cortical interneurons (Figures 6 and S5). Thus, we propose that *Shh* expression in the MGE MZ, by promoting expression of *Nkx2-1*, *Nkx6-2*, *Lhx6*, and *Lhx8* in the rostrodorsal MGE (Figures 4–6 and S4–S6), may equally drive production and/or survival of SOM^{+} and PV^{+} cortical interneurons. The *Dlx1/2-cre;Shh*$^{F/-}$ mutant also have reduced numbers of CR^{+} interneurons; we suggest that these largely correspond to the SOM^{+};CR^{+} subtype. On the other hand, we did not detect a change in NPY^{+} interneuron numbers, consistent with evidence that *Lhx6* is not essential in their generation (Zhao et al., 2008).

Finally, we propose that *Shh* expression in neurons of the rostrodorsal MGE and septum is required for the development of subpallial cell types in the anterior extension of the bed nucleus of stria terminalis (medial division; STMA), the core of the nucleus accumbens (AcbC), the lateral septum and the diagonal band complex (VDB/HBD), whereas the ventral pallidum, substantia inmoninata, and globus pallidus appeared normal (Figures 6 and S6). Future studies are needed to determine whether loss of Shh in the MGE MZ affects other aspects of its development such as guidance of axons that project to the pallidum (Charron et al., 2003).

LHX6 and LHX8 Bind to and Activate Transcription from a *Shh* MGE Enhancer

The loss of *Shh* expression in neurons of the MGE MZ in the *Lhx6*$^{PLAP/PLAP}$*;Lhx8*$^{-/-}$ mutant suggests that these transcription factors could directly regulate the *Shh* gene expression. We established using EMSA assays that LHX6 and LHX8 bind to a specific site in the SBE3 *shh* enhancer (ECR3) (Figure 8); SBE3 is a regulatory element that is specifically active in the MGE MZ (Jeong et al., 2006). Furthermore, *Lhx6* and *Lhx8* drive expression from the SBE3 *Shh* enhancer in MGE neurons (Figure 8). The transcriptional activation was context specific; while the SBE3 *Shh* enhancer was activated by *Lhx6* and *Lhx8* in MGE primary cultures, it was not activated in two tissue culture cell lines (P19 and HEK293T) (data not shown). Currently, we do not have antibodies that are effective for chromatin precipitation, and therefore cannot provide corroborative evidence for in vivo binding of LHX6 and LHX8 to the SBE3 *Shh* enhancer.

Shh Feed-Forward Signaling Cascade in the MGE Regulated by *Nkx2-1* and *Lhx6&8*

The results presented herein show novel evidence that SHH signaling provides a feed-forward cascade to regulating patterning, neural differentiation, and survival in the MGE (Figure 8E).

The scaffold of a genetic and biochemical pathway that drives development of the rostroventral telencephalon is now apparent. Induction of this region depends on FGF8 and SHH signaling; the former from the rostral patterning center (Storm et al., 2006) and the latter presumably from the hypothalamic anlage (Ohkubo et al., 2002). Embryos lacking *Fgf8* fail to induce *Nkx2-1* and *Shh* expression in the POA/MGE and express reduced levels of *Six3* and *Foxg1* (Storm et al., 2006); embryos lacking *Shh* fail to express *Nkx2-1* and do not maintain *Fgf8* expression (Ohkubo et al., 2002). *Nkx2-1* and *Foxg1* are each required in establishing *Shh* expression in the MGE/POA (Sussel et al., 1999; Geng et al., 2008; Manuel et al., 2010). *Nkx2-1* has a central role in specifying MGE identity (Sussel et al., 1999;

NIH-PA Author Manuscript

NIH-PA Author Manuscript

NIH-PA Author Manuscript

Flandin et al., 2010). In turn, *Shh* expression from the VZ of the MGE/POA is required to maintain normal levels of *Nkx2-1* (Xu et al., 2005, 2010; Gulacsi and Anderson, 2006), which then drives *Lhx6* and *Lhx8* expression (Sussel et al., 1999; Du et al., 2008). *Lhx6* and *Lhx8* are essential to activate *Shh* expression in early-born neurons of the MGE MZ (Figure 1), which then feeds-forward to regulate the identity, differentiation, survival, and late proliferation of the dorsal MGE by promoting expression of *Gli1*, *Nkx2-1*, *Nkx6-2*, and *Ptc1* (Figures 4, 5, S5, and S6). The affected derivatives of the dorsal MGE include pallial interneurons and components of the septum and bed nucleus stria terminalis (Figures 5–7). *Lhx6* and *Lhx8* are also essential to program the development of most MGE-derived projection neurons (e.g., globus pallidus and diagonal band) and interneurons (pallial and striatal) (Figures 2 and 3), through driving expression of *Lmo3* and *Nkx2-1* in the SVZ (Figure 2) and perhaps through maintaining *Sox6* expression in migrating interneurons (Figures 2 and 3) Finally, we propose that *Lhx6* and *Lhx8* prevent *Nkx2-1* expression in some pallial interneurons (Figures 3, S3, and 8E).

EXPERIMENTAL PROCEDURES

See Supplemental Experimental Procedures for detailed description of methods.

Mice

Lhx6$^{+/PLAP}$ mice were provided by Regeneron; they were generated and genotyped according to Choi et al. (2005). The *Lhx8* wild-type allele was genotyped as described in Zhao et al. (1999). *Shh*$^{F/F}$ mice (Dassule et al., 2000) were crossed with *Dlx1/2-cre* animals (Potter et al., 2009). Animals were treated in accordance with the protocols approved by the NICHD and UCSF Animal Use Committees.

Histology

In situ RNA hybridization experiments were performed using digoxigenin ribo-probes on 20 μm frozen sections as previously described (Cobos et al., 2007).

Immunofluorescence staining was performed according to Flandin et al. (2010).

PLAP expression was assayed as in Shah et al. (2004).

Transcription Activation Assays in Primary MGE Cell Cultures

The MGE (progenitor and mantle zones) was dissected from E12.5 CD-1 wild-type embryos. Twenty-four hours after seeding, cells were transfected using Fugene6 (Roche) with various combinations of mCherry reporter vectors (SBE3-wtA or SBE3-mutA) and transcription factor vectors (*Lhx6* and/or 3xFLAG-*Lhx8*). mCherry protein expression was detected 48 hr after transfection by immunofluorescence. The number of mCherry^{+} cells was measured and represented in Figure 8C as the mean ± SEM from four independent experiments.

Electrophoretic Mobility Shift Assay (EMSA)

EMSA was performed using the kit from Pierce. Briefly, each reaction (20 μl) consisted of ~2 μg nuclear extract, 1 fmol/μl of biotinylated probes, with or without cold competitor probe (200, 50, or 10 fmol/μl) in binding buffer consisting of 10 mM Tris (pH 7.5), 50 mM KCl, 1 mM DTT, 5% glycerol, 1 mM EDTA, 50 ng/μl poly (dI-dC) (Sigma), and 50 ng/μl bovine serum albumin (New England Biolabs).

LHX6, LHX8, and LDB1 proteins were generated by Fugene6 transfection of HEK293 cells. After 48 hr, nuclear extracts were prepared using the Pierce nuclear extract kit.

NIH-PA Author Manuscript

NIH-PA Author Manuscript

NIH-PA Author Manuscript

Biotinylated DNA probes were as follows: probe A corresponded to the 26–64 bp of the SBE3 *Shh* enhancer and included LHX site A (Figure 8A); mutated probe A had the same nucleotide sequence as the wild-type probe A, but the LHX site core sequence (TAATCA) changed to TTTTTT.

Supplementary Material

Refer to Web version on PubMed Central for supplementary material.

Acknowledgments

This work was supported by the research grants to J.L.R.R. from Nina Ireland, Larry L. Hillblom Foundation, March of Dimes, Weston Havens Foundation, NIMH R37 MH049428 and R01 MH081880; to J.J. from NIDCR K99 DE019486-01; and to H.W. and Y.Z. from the intramural research program of the Eunice Kennedy Shriver National Institute of Child Health and Human Development/NIH.

REFERENCES

Alifragis P, Liapi A, Parnavelas JG. Lhx6 regulates the migration of cortical interneurons from the ventral telencephalon but does not specify their GABA phenotype. J. Neurosci. 2004; 24:5643–5648. [PubMed: 15201337]

Azim E, Jabaudon D, Fame RM, Macklis JD. SOX6 controls dorsal progenitor identity and interneuron diversity during neocortical development. Nat. Neurosci. 2009; 12:1238–1247. [PubMed: 19657336]

Batista-Brito R, Fishell G. The developmental integration of cortical interneurons into a functional network. Curr. Top. Dev. Biol. 2009; 87:81–118. [PubMed: 19427517]

Batista-Brito R, Rossignol E, Hjerling-Leffler J, Denaxa M, Wegner M, Lefebvre V, Pachnis V, Fishell G. The cell-intrinsic requirement of Sox6 for cortical interneuron development. Neuron. 2009; 63:466–481. [PubMed: 19709629]

Butt SJ, Sousa VH, Fuccillo MV, Hjerling-Leffler J, Miyoshi G, Kimura S, Fishell G. The requirement of Nkx2-1 in the temporal specification of cortical interneuron subtypes. Neuron. 2008; 59:722–732. [PubMed: 18786356]

Charron F, Stein E, Jeong J, McMahon AP, Tessier-Lavigne M. The morphogen sonic hedgehog is an axonal chemoattractant that collaborates with netrin-1 in midline axon guidance. Cell. 2003; 113:11–23. [PubMed: 12679031]

Choi GB, Dong HW, Murphy AJ, Valenzuela DM, Yancopoulos GD, Swanson LW, Anderson DJ. Lhx6 delineates a pathway mediating innate reproductive behaviors from the amygdala to the hypothalamus. Neuron. 2005; 46:647–660. [PubMed: 15944132]

Cobos I, Borello U, Rubenstein JL. Dlx transcription factors promote migration through repression of axon and dendrite growth. Neuron. 2007; 54:873–888. [PubMed: 17582329]

Dassule HR, Lewis P, Bei M, Maas R, McMahon AP. Sonic hedgehog regulates growth and morphogenesis of the tooth. Development. 2000; 127:4775–4785. [PubMed: 11044393]

Du T, Xu Q, Ocbina PJ, Anderson SA. NKX2.1 specifies cortical interneuron fate by activating Lhx6. Development. 2008; 135:1559–1567. [PubMed: 18339674]

Flames N, Pla R, Gelman DM, Rubenstein JLR, Puelles L, Marín O. Delineation of multiple subpallial progenitor domains by the combinatorial expression of transcriptional codes. J. Neurosci. 2007; 27:9682–9695. [PubMed: 17804629]

Flandin P, Kimura S, Rubenstein JL. The progenitor zone of the ventral medial ganglionic eminence requires Nkx2-1 to generate most of the globus pallidus but few neocortical interneurons. J. Neurosci. 2010; 30:2812–2823. [PubMed: 20181579]

Fragkouli A, Hearn C, Errington M, Cooke S, Grigoriou M, Bliss T, Stylianopoulou F, Pachnis V. Loss of forebrain cholinergic neurons and impairment in spatial learning and memory in LHX7-deficient mice. Eur. J. Neurosci. 2005; 21:2923–2938. [PubMed: 15978004]

NIH-PA Author Manuscript

NIH-PA Author Manuscript

NIH-PA Author Manuscript

Fragkouli A, van Wijk NV, Lopes R, Kessaris N, Pachnis V. LIM homeodomain transcription factor-dependent specification of bipotential MGE progenitors into cholinergic and GABAergic striatal interneurons. Development. 2009; 136:3841–3851. [PubMed: 19855026]

García-López M, Abellán A, Legaz I, Rubenstein JL, Puelles L, Medina L. Histogenetic compartments of the mouse centromedial and extended amygdala based on gene expression patterns during development. J. Comp. Neurol. 2008; 506:46–74. [PubMed: 17990271]

Geng X, Speirs C, Lagutin O, Inbal A, Liu W, Solnica-Krezel L, Jeong Y, Epstein DJ, Oliver G. Haploinsufficiency of Six3 fails to activate Sonic hedgehog expression in the ventral forebrain and causes holoprosencephaly. Dev. Cell. 2008; 15:236–247. [PubMed: 18694563]

Gulacsi A, Anderson SA. Shh maintains Nkx2.1 in the MGE by a Gli3-independent mechanism. Cereb. Cortex. 2006; 16(Suppl 1):i89–i95. [PubMed: 16766713]

Jeong Y, El-Jaick K, Roessler E, Muenke M, Epstein DJ. A functional screen for sonic hedgehog regulatory elements across a 1 Mb interval identifies long-range ventral forebrain enhancers. Development. 2006; 133:761–772. [PubMed: 16407397]

Lavdas AA, Grigoriou M, Pachnis V, Parnavelas JG. The medial ganglionic eminence gives rise to a population of early neurons in the developing cerebral cortex. J. Neurosci. 1999; 19:7881–7888. [PubMed: 10479690]

Lewis PM, Gritli-Linde A, Smeyne R, Kottmann A, McMahon AP. Sonic hedgehog signaling is required for expansion of granule neuron precursors and patterning of the mouse cerebellum. Dev. Biol. 2004; 270:393–410. [PubMed: 15183722]

Liodis P, Denaxa M, Grigoriou M, Akufo-Addo C, Yanagawa Y, Pachnis V. Lhx6 activity is required for the normal migration and specification of cortical interneuron subtypes. J. Neurosci. 2007; 27:3078–3089. [PubMed: 17376969]

Machold R, Hayashi S, Rutlin M, Muzumdar MD, Nery S, Corbin JG, Gritli-Linde A, Dellovade T, Porter JA, Rubin LL, et al. Sonic hedgehog is required for progenitor cell maintenance in telencephalic stem cell niches. Neuron. 2003; 39:937–950. [PubMed: 12971894]

Manuel M, Martynoga B, Yu T, West JD, Mason JO, Price DJ. The transcription factor Foxg1 regulates the competence of telencephalic cells to adopt subpallial fates in mice. Development. 2010; 137:487–497. [PubMed: 20081193]

Marín O, Rubenstein JL. A long, remarkable journey: tangential migration in the telencephalon. Nat. Rev. Neurosci. 2001; 2:780–790. [PubMed: 11715055]

Marín O, Anderson SA, Rubenstein JL. Origin and molecular specification of striatal interneurons. J. Neurosci. 2000; 20:6063–6076. [PubMed: 10934256]

Mori T, Yuxing Z, Takaki H, Takeuchi M, Iseki K, Hagino S, Kitanaka J, Takemura M, Misawa H, Ikawa M, et al. The LIM homeobox gene, L3/Lhx8, is necessary for proper development of basal forebrain cholinergic neurons. Eur. J. Neurosci. 2004; 19:3129–3141. [PubMed: 15217369]

Nóbrega-Pereira S, Kessaris N, Du T, Kimura S, Anderson SA, Marín O. Postmitotic Nkx2-1 controls the migration of telencephalic interneurons by direct repression of guidance receptors. Neuron. 2008; 59:733–745. [PubMed: 18786357]

Nóbrega-Pereira S, Gelman D, Bartolini G, Pla R, Pierani A, Marín O. Origin and molecular specification of globus pallidus neurons. J. Neurosci. 2010; 30:2824–2834. [PubMed: 20181580]

Ohkubo Y, Chiang C, Rubenstein JL. Coordinate regulation and synergistic actions of BMP4, SHH and FGF8 in the rostral prosencephalon regulate morphogenesis of the telencephalic and optic vesicles. Neuroscience. 2002; 111:1–17. [PubMed: 11955708]

Potter GB, Petryniak MA, Shevchenko E, McKinsey GL, Ekker M, Rubenstein JLR. Generation of Cre-transgenic mice using Dlx1/Dlx2 enhancers and their characterization in GABAergic interneurons. Mol. Cell. Neurosci. 2009; 40:167–186. [PubMed: 19026749]

Shah NM, Pisapia DJ, Maniatis S, Mendelsohn MM, Nemes A, Axel R. Visualizing sexual dimorphism in the brain. Neuron. 2004; 43:313–319. [PubMed: 15294140]

Sousa VH, Miyoshi G, Hjerling-Leffler J, Karayannis T, Fishell G. Characterization of Nkx6-2-derived neocortical interneuron lineages. Cereb. Cortex. 2009; 19(Suppl 1):i1–i10. [PubMed: 19363146]

NIH-PA Author Manuscript

NIH-PA Author Manuscript

NIH-PA Author Manuscript

Storm EE, Garel S, Borello U, Hebert JM, Martinez S, McConnell SK, Martin GR, Rubenstein JL. Dose-dependent functions of Fgf8 in regulating telencephalic patterning centers. Development. 2006; 133:1831–1844. [PubMed: 16613831]

Sussel L, Marin O, Kimura S, Rubenstein JL. Loss of Nkx2.1 homeobox gene function results in a ventral to dorsal molecular respecification within the basal telencephalon: evidence for a transformation of the pallidum into the striatum. Development. 1999; 126:3359–3370. [PubMed: 10393115]

Wonders CP, Anderson SA. The origin and specification of cortical interneurons. Nat. Rev. Neurosci. 2006; 7:687–696. [PubMed: 16883309]

Wonders CP, Taylor L, Welagen J, Mbata IC, Xiang JZ, Anderson SA. A spatial bias for the origins of interneuron subgroups within the medial ganglionic eminence. Dev. Biol. 2008; 314:127–136. [PubMed: 18155689]

Xu Q, Wonders CP, Anderson SA. Sonic hedgehog maintains the identity of cortical interneuron progenitors in the ventral telencephalon. Development. 2005; 132:4987–4998. [PubMed: 16221724]

Xu Q, Guo L, Moore H, Waclaw RR, Campbell K, Anderson SA. Sonic hedgehog signaling confers ventral telencephalic progenitors with distinct cortical interneuron fates. Neuron. 2010; 65:328–340. [PubMed: 20159447]

Yu W, Wang Y, McDonnell K, Stephen D, Bai CB. Patterning of ventral telencephalon requires positive function of Gli transcription factors. Dev. Biol. 2009; 334:264–275. [PubMed: 19632216]

Zhao Y, Guo YJ, Tomac AC, Taylor NR, Grinberg A, Lee EJ, Huang S, Westphal H. Isolated cleft palate in mice with a targeted mutation of the LIM homeobox gene lhx8. Proc. Natl. Acad. Sci. USA. 1999; 96:15002–15006. [PubMed: 10611327]

Zhao Y, Marín O, Hermesz E, Powell A, Flames N, Palkovits M, Rubenstein JL, Westphal H. The LIM-homeobox gene Lhx8 is required for the development of many cholinergic neurons in the mouse forebrain. Proc. Natl. Acad. Sci. USA. 2003; 100:9005–9010. [PubMed: 12855770]

Zhao Y, Flandin P, Long JE, Cuesta MD, Westphal H, Rubenstein JL. Distinct molecular pathways for development of telencephalic interneuron subtypes revealed through analysis of Lhx6 mutants. J. Comp. Neurol. 2008; 510:79–99. [PubMed: 18613121]

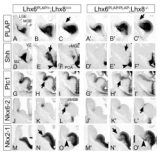

Figure 1. *Lhx6*$^{PLAP/PLAP}$;*Lhx8*$^{-/-}$ Double Mutants Fail to Express *Shh* in Neurons of the E11.5 MGE Mantle Zone (MZ) and Have Reduced Shh Signaling in the Proliferative Zone of the Dorsal MGE

The genotype of the control embryo was *Lhx6*$^{PLAP/+}$;*Lhx8*$^{+/+}$. Subpallial images of E11.5 three serial coronal hemisections (rostral-most on the left) show the preservation of Lhx6-placental alkaline phosphatase (PLAP) expression (A–C and A′–C′) or in situ RNA hybridization staining for *Shh* (D–F and D′–F′), *Ptc1* (G–I and G′–I′), *Nkx6-2* (J–L and J′–L′), and *Nkx2-1* (M–O and M′–O′). Arrows in (C) and (C′) show the reduced PLAP^{+} tangentially migrating cells in the mutant. Arrows in (E) and (E′) indicate the lack of Shh expression in the mantle region of the MGE of the mutant whereas *Shh* expression in the ventricular zone (VZ) of the ventral MGE and POA is not affected (arrowheads). Arrows in (H) and (H′) indicate the reduction in *Ptc1* expression in the VZ of the dorsal MGE of the mutant. Arrows in (L) and (L′) indicate the reduction of *Nkx6-2* expression in the dorsal-most MGE (sulcus between LGE and MGE). Arrows in (N) and (N′) indicate lack of *Nkx2-1* expression in the dorsal MGE, and arrowheads in (O) and (O′) show ectopic expression of *Nkx2-1* in the superficial MZ of the MGE. Abbreviations: LGE, lateral ganglionic eminence; MGE, medial ganglionic eminence; dMGE dorsal MGE; vMGE, ventral MGE; MZ, mantle zone; POA, preoptic area. Scale bar: 500 μm. See also Figure S1 and Table S1.

NIH-PA Author Manuscript NIH-PA Author Manuscript NIH-PA Author Manuscript

NIH-PA Author Manuscript

NIH-PA Author Manuscript

NIH-PA Author Manuscript

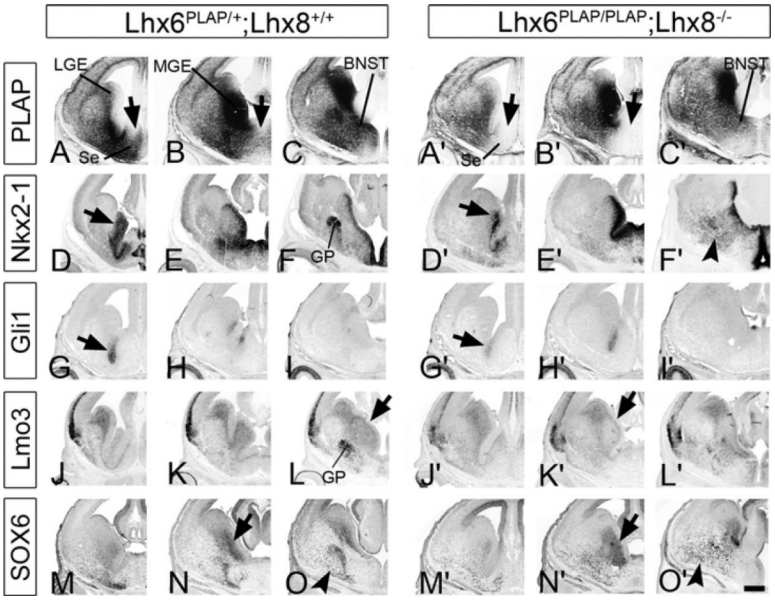

Figure 2. Molecular Defects in the Ventral Telencephalon of the *Lhx6*$^{PLAP/PLAP}$;*Lhx8*$^{-/-}$ Double Mutant at E14.5

The genotype of the control embryo was *Lhx6*$^{PLAP/+}$;*Lhx8*$^{+/+}$. MGE images of three serial coronal hemisections (rostral-most on the left) show Lhx6-PLAP expression (A–C and A′–C′) and in situ RNA hybridization staining for *Nkx2-1* (D–F and D′–F′), *Gli1* (G–I and G′–I′), *Lmo3* (J–L and J′–L′), and immunofluorescence using an antibody to SOX6 (M–O and M′–O′). Arrows in (D) and (D′) indicate the reduction in *Nkx2-1* expression in the SVZ of the MGE of the double mutant. Arrows in (L) and (K′) indicate lack of Lmo3 in the SVZ of the MGE of the double mutant. Arrows in (N) and (N′) indicate maintenance of SOX6 expression in the SVZ of the MGE, and arrowheads in (F′) and (O′) indicate ectopic Nkx2-1^{+} and SOX6^{+} cells scattered in the MZ of the caudoventral telencephalon in the double mutant, respectively. Abbreviations: BNST, bed nucleus stria terminalis; GP, globus pallidus; LGE, lateral ganglionic eminence; MGE, medial ganglionic eminence; Se, septum. Scale bar: 500 μm. See also Figure S2 and Table S2.

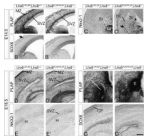

Figure 3. Cortical Interneuron Defect in the *Lhx6*$^{PLAP/PLAP}$;*Lhx8*$^{-/-}$ Double Mutant at E14.5 and E18.5

The genotype of the control embryo was *Lhx6*$^{PLAP/+}$;*Lhx8*$^{+/+}$. E14.5 cortex and LGE stained for *Lhx6*-PLAP activity (A and A′), SOX6 (B and B′), and *Nkx2-1* (C and C′). Note the severe reduction of *Lhx6*-PLAP^{+} and SOX6^{+} cells in the MZ (arrow), whereas the SVZ is less affected (A and A′; B and B′). Also note the ectopic *Nkx2-1*$^{+}$ cells in the ventrolateral cortex and external capsule (EC; arrow in C), and the increase numbers in the striatum (arrowhead in C′). E18.5 neocortex and hippocampus stained for *Lhx6*-PLAP activity (D and D′; F and F′), or immunostaining for NKX2-1 (E and E′) and SOX6 (G and G′). Note the severe reduction of PLAP staining in most of the neocortex (except the SVZ), but its preservation in the hippocampus (D and D′); the regions with preserved PLAP expression coincide with regions containing ectopic NKX2-1^{+} cells (E and E′). (F) and (F′) illustrate an ectopic collection (E) of *Lhx6*-PLAP expressing cells in SVZ of the MGE of the double mutant at E18.5, suggesting a defect in cell migration. Abbreviations: CP, cortical plate; EC, external capsule; E, ectopia; GP, globus pallidus; H, hippocampus; MZ, marginal zone; St, striatum; SVZ, subventricular zone. Scale bar: 200 μm. See also Figure S3 and Table S2.

NIH-PA Author Manuscript NIH-PA Author Manuscript NIH-PA Author Manuscript

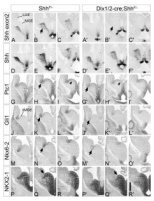

Figure 4. Molecular Defects in the MGE of the *Dlx1/2-cre*;*Shh*$^{F/-}$ Mutant at E11.5

The genotype of the control embryo was *Shh*$^{F/-}$. MGE images of three serial coronal hemisections (rostral-most on the left) show in situ RNA hybridization staining for Shh exon 2 (A–C and A′–C′), *Shh* (640 bp covering most of the coding region) (D–F and D′–F′), *Ptc1* (G–I and G′–I′), *Gli1* (J–L and J′–L′), and *Nkx6-2* (M–O and M′–O′), and NKX2-1 immunostaining (P–R and P′–R′). Note the loss of *Shh* exon2 expression in the MGE MZ (arrows in B and B′), but its maintenance in the MGE VZ (arrowheads in C and B′), and the reduced expression of *Ptc1*, *Gli1*, and *Nkx6-2* in the VZ of the dorsal MGE (arrows in H and G′, K and J′, and N and M′); NKX2-1 expression was only reduced in a small dorsal MGE region (arrows in Q and Q′). Abbreviations: LGE, lateral ganglionic eminence; MGE, ventral medial ganglionic eminence; dMGE, dorsal MGE. Scale bar: 400 μm. See also Figure S4 and Table S1.

NIH-PA Author Manuscript NIH-PA Author Manuscript NIH-PA Author Manuscript

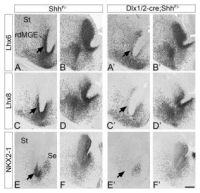

Figure 5. Molecular Defects in the MGE of *Dlx1/2-cre*;*Shh*$^{F/-}$ Mutant at E14.0

The genotype of the control embryo was *Shh*$^{F/-}$. MGE images of two serial coronal hemisections (rostral-most on the left) show in situ RNA hybridization staining for *Lhx6* (A and B; A′ and B′) and *Lhx8* (C and D; C′ and D′), and NKX2-1 immunostaining (E and F; E′ and F′). Note the reduction in *Lhx6*, *Lhx8*, and NKX2-1 expression in the VZ, SVZ, and MZ of the rostrodorsal MGE and ventral septum of the mutant (arrows). Abbreviations: rdMGE, rostrodorsal medial ganglionic eminence; Se, septum; St, striatum. Scale bar: 200 μm. See also Figure S5 and Table S3.

NIH-PA Author Manuscript NIH-PA Author Manuscript NIH-PA Author Manuscript

NIH-PA Author Manuscript
NIH-PA Author Manuscript
NIH-PA Author Manuscript

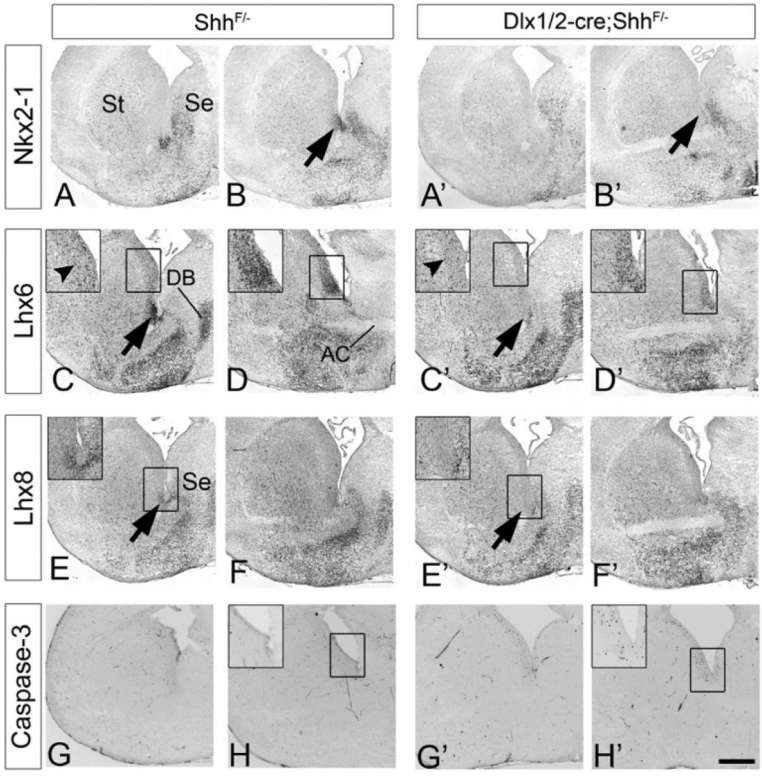

Figure 6. Molecular Defects in the Rostral Basal Ganglia (Striatal and Septal Regions) of *Dlx1/2-cre;Shh*$^{F/-}$ Mutant at E18.5

The genotype of the control embryo was Shh$^{F/-}$. Two serial coronal hemisections (rostral-most on the left) show in situ RNA hybridization staining for *Nkx2-1* (A and B; A′ and B′), *Lhx6* (C and D; C′ and D′) and *Lhx8* (E and F; E′ and F′). Note the reduction in *Nkx2-1*, *Lhx6*, and *Lhx8* expression in the VZ, SVZ and MZ of the rostrodorsal MGE (arrow) and ventrolateral septum of the mutant. Increased apoptosis (activated Caspase-3) in the *Dlx1/2-cre*;*Shh*$^{F/-}$ mutant compare to the control (G and H; G′ and H′); boxed regions are 2-fold higher magnification. Abbreviations: AC, anterior commissure; DB, diagonal band; Se, septum; St, striatum. Scale bar: 500 μm. See also Figure S6 and Table S3.

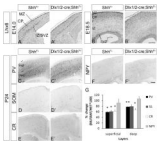

Figure 7. Molecular Defects in the Neocortex of *Dlx1/2-cre*;*Shh*$^{F/-}$ Mutant at E14.0, E18.5, and P24

The genotype of the control embryo was *Shh*$^{F/-}$. Coronal hemisections show in situ RNA hybridization staining for *Lhx6* at E14.0 (A and A′) and E18.5 (B and B′). Coronal sections from 24-day-old mice were stained using PV (C and C′), SOM (D and D′), CR (E and E′), and NPY (F and F′) antibodies. The graph in (G) summarizes the reduction in PV$^+$, SOM$^+$, and CR$^+$ cells in the superficial (Sup) and deep layers of the somatosensory cortex. NPY$^+$ cells were not reduced. Data are the mean ± SEM. *$p < 0.05$; **$p < 0.01$ (paired Student's t test; see Experimental Procedures). Abbreviations: CP, cortical plate; IZ, intermediate zone; MZ, marginal zone; Sup, superficial; St, striatum; SVZ, subventricular zone. Scale bar: 100 μm for (A)–(B′) and 400 μm for (C)–(F′). See also Table S3.

NIH-PA Author Manuscript NIH-PA Author Manuscript NIH-PA Author Manuscript

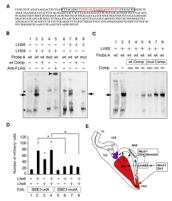

Figure 8. LHX6 and LHX8 Can Bind to and Regulate the *Shh* Enhancer (SBE3)

(A) Sequence of SBE3. The predicted LHX-binding sequence is shown in red and its core region (TAATCA) is underlined. A box shows the region called probe A used in EMSA assays (below).

(B) Electrophoretic mobility shift assay showing that LHX6 and LHX8 bind to the SBE3 *Shh* enhancer. DNA binding assay, using LHX6- or LHX8-containing nuclear extracts, results in a probe A-protein complex (arrows; lanes 2 and 7), compared to control extract (lanes 1 and 6; two "LHX site A nonspecific" bands; asterisks). When 200-fold mole excess unbiotinylated wild-type (WT) probe A (WT competitor [Comp]) was added to the binding assay, the DNA/protein complexes were nearly eliminated (lanes 3 and 8). On the other hand, biotinylated mutant (mut) probe A (LHX site A core sequence changed from TAATCA to TTTTTT) prevented the formation of the LHX-specific complex (arrows) (lanes 4 and 9). Addition of anti-FLAG antibody to the 3× FLAG-tagged LHX8/WT probe A binding reaction resulted in a supershift of the LHX8-probe A complex (arrowhead; lane 5).

(C) Titration of wild-type competitor A (lanes 3, 4, 5) and mutant competitor A (lanes 6, 7, 8) in LHX8 EMSA competition assays. Nuclear extracts from control (lane 1) and LHX8 transfected (lanes 2–8) cells. LHX8-probe A complex (arrow) formation was differentially reduced using 200-fold, 50-fold, and 10-fold mole excess of either WT or mutant unbiotinylated probe A. Ten-fold excess unbiotinylated WT probe A (lane 5) resulted in a similar reduction to 200-fold unbiotinylated mutant probe A (lane 6).

(D) *Lhx6* and *Lhx8* can activate transcription from the SBE3 *Shh* enhancer. Lanes 1–4: dissociated E12.5 MGE cells cotransfected with a WT *Shh* enhancer (SBE3-wtA) driving *mCherry* expression with expression vectors that drive expression of *Lhx6*, *Lhx8*, or a 1:1 mixture of *Lhx6*&*8*. Each transfection condition was analyzed by immunofluorescence for expression of mCherry. All three conditions induced a 3- to 5-fold increase in mCherry expression (red asterisks: statistical significance compare to control). Lanes 5–8: MGE cells cotransfected with the mutant SBE3 *Shh* enhancer driving *mCherry* (SBE3-mutA; see above in A); in this case *Lhx6*, *Lhx8*, and *Lhx6*&*8* resulted in a slight (not statistically significant) increase in mCherry. Mutation of the LHX site in SBE3 resulted in ~2.5 reduced *Lhx6*- and *Lhx6*&*8*-mediated expression (black asterisks). Data are the mean ± SEM. n = 4; *$p < 0.05$ (two-tailed unpaired Student t test).

(E) Schema summarizing results described in the paper, and hypothesized regulatory cascades (see Discussion). Abbreviations: Cx, cortex; LGE, lateral ganglionic eminence; MGE, medial ganglionic eminence; MZ, mantle zone; POA, preoptic area.

NIH-PA Author Manuscript NIH-PA Author Manuscript NIH-PA Author Manuscript